doi: 10.30934/kusbed.666084 **e-ISSN:** 2149-8571

Kocaeli Üniversitesi Sağlık Bilimleri Dergisi

Özgün Araştırma / Original Article

http://dergipark.gov.tr/kusbed

CHANGES OCCURRING IN THE PROTEOME OF SH-SY5Y CELLS CAUSED BY FAT MASS AND OBESITY ASSOCIATED (FTO) PROTEIN EXPRESSION REVEALS MULTIFACETED PROPERTIES OF THE FTO PROTEIN

FAT MASS AND OBESITY ASSOCIATED (FTO) PROTEİN EKSPRESYONUNUN NEDEN OLDUĞU SH-SY5Y HÜCRELERİNİN PROTEOMUNDA MEYDANA GELEN DEĞİŞİKLİKLER, FTO PROTEİNİNİN ÇOK YÖNLÜ ÖZELLİKLERİNİ ORTAYA ÇIKARIR

Aylin Kanlı[1*], Murat Kasap[1], Gürler Akpınar[1], Sevinç Yanar[1]

[1]Kocaeli University, Faculty of Medicine, Department of Medical Biology, Kocaeli, Turkey

ORCID iD: Aylin Kanlı: 0000-0002-0674-0072; Murat Kasap: 0000-0001-8527-2096; Gürler Akpınar: 0000-0002-9675-3714; Sevinç Yanar: 0000-0002-6438-7385

***Sorumlu Yazar / Corresponding Author:** Aylin Kanlı, **e-posta / e-mail:** aylin.kanli@kocaeli.edu.tr

Geliş Tarihi / Received: 27.12.2019 **Kabul Tarihi / Accepted:** 23.04.2020 **Yayım Tarihi / Published:** 05.06.2020

Abstract

Objective: Fat mass and obesity associated (FTO) protein is an RNA-demethylase which is employed in various metabolic functions such as post-transcriptional modifications, DNA repair and fatty acid utilization. Fat mass and obesity associated protein was initially found to be closely associated with obesity and increased body-mass-index and later studies have established association of FTO with neurological diseases and cancer. The aim of this study was to investigate the effect of R316Q FTO mutation on soluble proteome in SH-SY5Y cells.
Methods: SH-SY5Y cells stably expressing the wild-type (WT) and the mutant FTO proteins under the control of Tet-promoter were used to study changes in overall proteome using two-dimentional Difference Gel Electrophoresis approach. More than 500 protein spots were compared in samples that overexpressed the WT-FTO or the mutant-FTO protein according to 2-fold-criteria. Spots displaying differences were cut from the gels and identified by MALDI-TOF/TOF.
Results: In overall, the expression of neither the WT nor the mutant FTO caused major changes in the soluble proteome. However, we observed some minor changes in six protein spots. Three of those protein spots belonged to Hsp70 and were up-regulated in the mutant-FTO-expressing cells. This indicated that Hsp70 was not only up-regulated but also post-translationally modified. The other proteins regulated were phosphoglycerate kinase-1, calmodulin and keratin.
Conclusion: These results indicated that FTO appear to be associated with energy metabolism and might induce the cellular stress. In addition, FTO might affect to the Wnt signalling pathway. In overall, our study highlighted the multifaceted properties of the FTO and reflected onto the changes occurring in the proteome of neuroblastoma cells.

Keywords: *Fat mass and obesity associated (FTO) protein, R316Q-mutation, FTO-related-diseases, SH-SY5Y, Proteomics, 2D-DIGE*

Öz

Amaç: Fat mass and obesity associated (FTO) proteini postranskripsiyonel modifikasyonlar, DNA tamiri ve yağ asidi metabolizması gibi çeşitli hücresel işlevlerde rol oynayan bir RNA dematilazdır. Başlangıçta obesite ile yakından ilişkilendirilen FTO proteininin daha sonraki çalışmalarla nörolojik hastalıklar ve çeşitli kanser türleri ile ilişkili olduğu gösterilmiştir. Bu çalışmanın amacı SH-SY5Y hücrelerinde FTO geninin ekzonik R316Q mutasyonunun çözünür proteom üzerindeki etkilerini araştırmaktır.
Yöntem: İki boyutlu Difference Gel Electrophoresis (2D-DIGE) deneylerinde, Tet promotörün kontrolü altında yabanıl (WT) veya mutant FTO proteinlerini stabil şekilde eksprese eden SH-SY5Y hücreleri kullanılmıştır. 2-kat regülasyon kriterine göre WT ve mutant FTO proteinini fazla eksprese eden örneklerde 500'den fazla protein spotu karşılaştırılmış ve ekspresyonlarında değişiklik görülen protein-spotları jellerden kesilerek MALDI-TOF/TOF ile tanımlanmıştır.
Bulgular: Genel olarak, WT ve mutant FTO ifadesi çözünür proteomda büyük değişikliklere neden olmamıştır. Ancak, altı protein noktasında bazı küçük değişiklikler gözlemledik. Bu protein noktalarının üçü Hsp70'e aitti ve mutant FTO eksprese eden hücrelerde daha fazla eksprese idi. Bu, Hsp70'in yalnızca fazla eksprese olduğunu değil, aynı zamanda translasyon sonrası değişikliğe uğradığını da gösterir. İfadesi regüle edilen diğer proteinler fosfogliserat kinaz-1 (PGK1), kalmodulin ve keratindir.
Sonuç: Bu sonuçlar FTO'nun enerji metabolizması ile ilişkisinin yanı sıra hücresel strese cevabı indükleyebileceğinin bir göstergesi olabilir. Ek olarak, FTO Wnt sinyal iletim yolağını etkiyelebilir. Genel olarak, çalışmamız FTO'nun çok yönlü özelliklerini vurgulamış ve nöroblastom hücrelerinin proteomunda meydana gelen değişiklikleri yansıtmıştır.

Anahtar Kelimeler: *Fat mass and obesity associated (FTO) proteini, R316Q mutasyonu, FTO-ilişkili hastalıklar, SH-SY5Y, Proteomiks, 2D-DIGE*

Introduction

Fat mass and obesity associated (FTO) protein is mainly a nuclear protein belonging to the AlkB related non-heme Fe(II)/2-OG-dependent oxidative DNA/RNA demethylase superfamily.[1-4] Several studies have been conducted on the function and the localization of the FTO.[1-11] Initial studies of FTO localization have been reported that a distinct nuclear localization for the FTO, without the possibility of its participation to secretory pathway to be targeted to the cellular membranes or to specific organelles.[1,2] Relatively recently, Gulati et al. demonstrated the existance of FTO in the cytoplasmic fractions when they performed cellular fractionation experiments.[5,6] Initial studies regarding the biologic activity of FTO firmly established that the protein displays 3-meT activity on DNA.[1] Later studies however revealed that its main substrate was RNA rather than DNA.[3,4] Fat mass and obesity associated protein preferentially displays demethylase activity on N6-methyl adenosine (m^6A) of single-stranded RNA molecules.[4] The nucleoside m^6A is an abundant modification in RNA and its demethylation by FTO appear to be highly significant in determining cell fate esp., in tissue development, cell renewal and differentiation, DNA damage response and cancer development.[4,7-9] Two recent studies attributed a novel and selective demethylation activity to FTO and concluded that FTO may target m^6A primarily in the nucleus and N^6,2′-O-dimethyladenosine (m^6Am) in the cytoplasm.[10,11] However, the physiological consequences of these two separate activites are yet to be discovered.[10, 11]

The clinical significance of FTO was recognized in earlier studies. Several genome wide association studies identified an association between common variants of the FTO gene and childhood and adult obesities.[12-15] Subsequent large-scale genotyping studies have shown that SNPs in FTO gene are associated with many diseases. Variants in the FTO gene have also been associated with neurological disease states such as depression,[16] Alzheimer's disease[17,18] and sporadic amyotrophic lateral sclerosis.[19,20] The obesity associated variants are mostly localized to the intron 1 of the FTO gene. Genetic variants at the FTO locus are strongly associated with obesity-related traits by regulating neighboring genes.[21] On the other hand, some of the loss-of-function mutations in FTO were associated with neurodegeneration. For example, the R316Q mutation is found to be responsible for recessive lethal syndromes such as postnatal growth retardation, microcephaly, psychomotor delay, brain deficits, cardiac defects and low bone mineral density.[22,23]

The multi-physiological aspects of FTO were more prominent when studies were carried out in mice and humans. Fat mass and obesity associated protein is found to be associated with metabolic diseases (obesity, Type 2 diabetes and polycystic ovary syndrome), cancers (melanoma, breast, endometrial, pancreatic, prostate, colorectal, lung and kidney cancers), brain diseases (brain volume deficits and Alzheimer's disease) and cardiovascular systems.[24] In overall, FTO appears to play a hub-like function by affecting many different metabolic events. How FTO affects these many different but perhaps associated metabolic events is a matter of investigation. In the literature, a single publication from our laboratory investigated the possible effects of exogenously expressed wild-type and the mutant (R316Q) FTO on the soluble proteome of 3T3-L1 cells to elucidate changes and associate them with adipogenesis. In this study, a similar approach was taken to investigate the changes at the proteome of SH-SY5Y cells expressing the wild-type and the mutant (R316Q) FTO. SH-SY5Y cells have long been used as a model cell-line to study neurodegeneration.[25] Our study was the first study that provided details about FTO and its association with neurodegenerative events. The results of this study revealed the changes in expression levels of Hsp70, PGK1, Calmodulin and Keratin. Bioinformatics analysis of the regulated proteins implied changes occurring in energy metabolism upon expression of either the WT or the mutant FTO proteins. Analysis of metabolic processes indicated the presence of a response to cellular stress. In addition, the Wnt signalling pathway might be affected by FTO. In overall, our study highlighted the multifaceted properties of the FTO and reflected onto the changes occurring in proteome of neuroblastoma cells.

Methods

Creation of Plasmid Constructs

Full-length cDNA of the human WT-FTO gene was cloned into pcDNA4/TO (Life Tech, USA) by reverse transcription as detailed in our previous publication.[26] The pcDNA4/TO clone for the mutant FTO (R316Q) was created by Site-Directed Mutagenesis using a commercial kit (Invitrogen, USA) with the primers GTTTTGGCCGGTTCACAACCTC AGTTTAGTTCCACCCACCG and CGGTGGGTGGAAC TAAACTGAGGTTGTGAACCGGCCAAAAC for forward and reverse sequences, respectively. *Hind*III and *Xho*I restriction sites were added to the 5' ends of the primer sequences to ease the directional cloning of the PCR products. The constructs were sequenced and in-frame FTO sequences were verified (Eurofins, DE).[27] For localization study, the wild type and the mutant-FTO genes were amplified with Fwd and Rev primers containing *Xho*I and *Xba*I restriction enzyme cutting sites, respectively, and cloned into the GFP-harboring pcDNA4/TO plasmid. These constructs were also sequenced and in-frame FTO sequences were verified (Eurofins, DE).

Creation of stable cell lines expressing the WT and the Mutant FTO proteins

SH-SY5Y cells were grown in EMEM supplemented with 10% (Vol/Vol) tetracycline reduced fetal bovine serum, 100U/mL penicillin-streptomycin and 2 mM L-glutamine at 37°C in a humidified 5% CO2 atmosphere. Creation of Tet-R+ stable SHSY5Y cell line was described by.[28,29] To create stable cell lines expressing the WT or the mutant FTO proteins, TetR+SH-SY5Y cells were transfected with pcDNA4/TO clones as detailed in Kasap et al.[30] Individual clones were isolated, grew and examined for FTO protein expression by Western blotting with an anti-FTO antibody (Santa Cruz, Dallas, TX). The WT-FTO expressing clones were created and labeled as clones #3, #5, #12 for the WT in our previous study.[31] Three of the screened colonies expressing the mutant FTO proteins were propagated and labeled as clones #2, #3, #5 for the mutant.

Fluorescence Microscopy

SH-SY5Y-WT-FTO and SH-SY5Y-mutant-FTO expressing cells were cultured under standard tissue culture conditions, as it was performed in our previous study.[26] Culture plates contained glass cover slips that allowed fluorescence imaging. After 24 hrs of FTO expression, cells were fixed with formaldehyde and stained for FTO with an anti-FTO antibody (Clone C-3 (sc-271713), Santa Cruz, USA). The

nuclei of the cells were stained with DAPI (Lifetech. USA). Coverslips were mounted in Mowiol before the analysis.[32] Imaging was performed with an inverted microscope (Olympus CKX41) using appropriate filter sets.

Cycloheximide chase analysis

To evaluate stability of the WT-FTO protein and its mutant counterpart, stable SH-SY5Y cells expressing the WT and the mutant FTO proteins cells were used. Cells were incubated with tetracycline for 12 hours. To evaluate the stability of FTO proteins cells were treated with 100 µg/ml CHX (Sigma-Aldrich Co., St Louis, MO, USA) for a specific time course. All cells were lysed in 2D-extraction buffer before being subjected to SDS-PAGE and immunoblotting analyses.

Preparation of protein extracts

The cells were washed three times with ice-cold PBS and homogenized in lysis buffer (30mM Tris, 7M Urea, 2M Thiourea, 5mM Magnesium acetate, 4% [w/v] CHAPS pH 8.5), by using 0.1mm stainless steel beads in a mechanical disruption device (Bullet Blender; NextAdvance, Troy, NY). Homogenates were centrifuged at 15 000 x g for 30min at 4°C to remove cell debris. Protein concentrations were determined by modified Bradford assay (BioRad, Hercules, CA) and protein extracts were aliquoted, snap-frozen in liquid nitrogen, and stored at −80°C.

Western Blot Analysis

Western blot analysis was performed using anti-FTO (Clone C-3 (sc-271713), Santa Cruz, USA), anti-Hsp70, (sc-59569, Santa Cruz, USA), and anti-beta actin (Santa Cruz, USA; ACTBD, sc-81178) antibodies as described by Kasap et al. (2015). [33] For the purpose of band analysis, ImageJ, a freely available software was used as described by Kasap et al.[34] The software is available at the National Institutes of Health and can be downloaded from http://rsb.info.nih.gov/ij/ download.html. ImageJ measures the integrated density of each band by outlining it and using the Analyze/Measure command. The values obtained were plotted with Microsoft Excel software.

Minimal Protein Labeling for DIGE

Cells from three biologic replicates were used for protein extraction. The extracts were prepared in minimal DIGE lysis buffer (7 M Urea, 2 M Thiourea, 30 mM Tris, and 5 mM $Mg(CH3COO)_2$, pH 9) and equal amounts of proteins were pooled to create three different pools which were labeled with Cy2, Cy3, or Cy5 according to the instructions provided by the supplier (Life Tech, USA). The whole labeling experiments were carried out in the dark. In short, 50 μg of protein sample was used in each labeling experiment. After adjusting the pH of the extracts to 8.5, CyDye DIGE minimal dyes were added directly to the samples and incubated at 4°C for 30 min. The reactions were stopped by adding 10 mM lysine. Labeled samples were then pooled and used in 2D experiments.

2D Gel Electrophoresis Experiments

For DIGE experiments, three sets of gels were produced. The labeled protein samples were loaded onto immobilized 11 cm, pH gradient strips (IPG) (pH 3–10) by passive rehydration. Separation based on isoelectric points was performed by a Protean Isoelectric Focusing Cell (Bio-Rad, USA). The following conditions were used for IEF: twenty min at 250V with a rapid ramp followed by 2 hours at 4000Vwith a slow ramp and 2.5 hours for 4000V with a rapid ramp until a total of 32000V/h was reached at 20°C. After isoelectric focusing, the strips were washed with buffer I (6M Urea, 375mM Tris-HCl pH 8.8, 2% SDS, 20% glycerol, 2% (w/v) DTT) for 30 min and then with buffer II (6 M Urea, 375 mM Tris-HCl pH 8.8, 2% SDS, 20% glycerol, 2.5% iodoacetamide (w/v)) for 30 min at room temperature in the dark and subjected to SDS-PAGE using TGX precast gels in a Dodeca gel running system (Bio-Rad, USA). In parallel to the DIGE experiment, a preparative 2D gel experiment was run to cut protein spots for identification. A total of 240 μg of protein (80 μg from each sample) was loaded for each separation.

Image Analysis and Spot Cutting

DIGE images were captured using appropriate filter sets with VersaDoc4000 MP (Bio-Rad, USA). PDQuest Advance 2D-analysis software (BioRad, USA) was used for comparative analysis of protein spots. Quantity of each spot was normalized by local regression model. The statistical significance of image analysis was determined by Student's t-test (statistical level of p<0.05 is significant). Gel spots significantly differed in expression (more than 2-fold) and were selected and excised from gels using ExQuest Spot cutter (Bio-Rad, USA) for protein identification. A manual editing tool was used to inspect the determined protein spots detected by the software. The 3D view of the selected spots for each group was created to perform visual comparison using PDQuest Advance 2D-analysis software. The software is run with default settings.

In-gel tryptic digestion and Protein Identification

Protein identification experiments were performed at Kocaeli University DEKART proteomics laboratory using ABSCIEX MALDI-TOF/TOF 5800 system. In-gel tryptic digestions of the proteins were performed using an In-gel Digestion Kit following the recommended protocol by the manufacturer (Pierce, USA). Before deposition onto a MALDI plate, all samples were desalted and concentrated with a 10 μL ZipTipC18 following the recommended protocol (Millipore, USA). Peptides were eluted in a volume of 1 μL using a concentrated solution of α-cyano-4-hydroxycinnamic acid (α-CHCA) in 50% acetonitrile and 0.1% trifluoroacetic acid in water and spotted onto the MALDI target plate. The TOF spectra were recorded in the positive ion reflector mode with a mass range from 400 to 2000 Da. Each spectrum was the cumulative average of 200 laser shots. The spectra were calibrated with the trypsin autodigestion ion peaks m/z (842.510 and 2211.1046) as internal standards. Ten of the strongest peaks of the TOF spectra per sample were chosen for MS/MS analysis. All of the Peptide Mass Fingerprints (PMFs) were searched in the MASCOT version 2.5 (Matrix Science) using a streamline software, ProteinPilot (ABSCIEX, USA), with the following criteria: Swissprot; species restriction to Homo sapiens enzyme of trypsin; at least five independent peptides matched; at most one missed cleavage site; MS tolerance set to ±50 ppm and MS/MS tolerance set to ±0.4Da; fixed modification being International carbamidomethyl (Cys) and variable modification being oxidation (Met); peptide charge of 1+; and being monoisotopic. Only significant hits, as defined by the MASCOT probability analysis (p<0.05), were accepted. Protein score is $-10 * \log(p)$ where p is the probability that the observed match is a random event. Protein score, which has a value of p<0.05, is considered significant hit. Protein scores are derived from ion scores as a nonprobabilistic basis for ranking protein hits.

STRING Analysis

The STRING database (http://stringdb.org) aims to provide a critical assessment and integration of protein-protein interactions, including direct (physical) as well as indirect (functional) associations. STRING analysis was performed at http://string-db.org.

Results

Cloning of the wild type and the mutant type FTO genes

The WT-FTO PCR product was cloned into the pcDNA4/TO expression vector and labeled as pcDNA4/TO-FTO-WT.[26] The pcDNA4/TO clone for the mutant FTO (R316Q) was created from the pcDNA4/TO vector harboring the FTO-WT gene by Site-Directed Mutagenesis.[27] The *E. coli* clone carrying the mutant FTO gene on a recombinant plasmid DNA was selected for plasmid DNA isolation. The isolated plasmid DNA was labeled as pcDNA4/TO-FTO-R316Q then digested with *Hind*III and *Xho*I enzymes to demonstrate the presence of the mutated FTO insert. (Figure 1A). Physical map for pcDNA4/TO-FTO-R316Q clone was depicted in Figure 1B. The insert DNA was sequenced to verify the presence of mutated bases (Iontek Inc, Istanbul). The sequences were subjected to multiple sequence alignment to assess the position of the mutated amino acids. (Figure 1C). For localization study, GFP fusion proteins for the WT and the mutant proteins were created via cloning of the corresponding DNA sequences into pCDNA4/TO-GFP vector. To verify the WT and the mutant FTO-GFP fusion protein-coding gene sequences, the recombinant plasmid DNAs were digested with *Xho*I and *Xba*I and the resulting the inserts were analysed using 1% etidium bromide agarose gel (data not shown).

Establishment of stable cell lines capable of expressing the wild type and the mutant FTO

The SH-SY5Y cell line expressing the WT-FTO under the control of Tet induction were previously created in our laboratory using the pcDNA4/TO-FTO-WT recombinant plasmid.[26] In this study, we used the T-rex system (Invitrogen, USA) to create stable SH-SY5Y cell line that expressed the mutant FTO under tetracycline control. In brief, SH-SY5Y-TetR+ cells were transfected with with pcDNA4/TO-FTO-R316Q to create 3 inducible stable clones (colonies #2, #3 and #5) expressing the mutant FTO protein. The expressions were screened by western blotting (Figure 2). After tetracycline induction, a considerable increase was observed at the mutant FTO levels. Before the induction, a weak band appeared on the blots. It is likely that the weak band was from the endogeneous FTO protein expressed by the SH-SY5Y cells.

Fluorescence Imaging of FTO

The localization of both the WT and the mutant FTO in SH-SY5Y cells were monitored with immunofluorescence. Prior to imaging, both proteins were expressed for 16 hours in SH-SY5Y cells grown on cover slips. Both the WT and the mutant FTO proteins were localized to the nucleus. A similar nuclear localization pattern was detected for the WT- and the R316Q mutant-FTO proteins (Figure 3).

Cycloheximide chase assay

Prior to assessing the stability of the FTO proteins, we determined the optimum FTO levels that would allow detection of the changes occurring during cyclohexamide chase. The results demonstrated that 12 hours of FTO expression was sufficient for chasing the changes at FTO levels (Figure 4A). After FTO expression for 12-hour, CHX was added to culture plates containing both the wild and the mutant type FTO genes. At certain time intervals (0, 6, 12, 18, 24, 48, 72 hours), cells were harvested and protein samples were prepared. Protein degradation was determined by western blotting (Figure 4B). Analysis of the western blots indicated that the mutant FTO displayed a similar stability pattern to the WT-FTO. Both proteins stayed in the cells without being exposed to a significant degredation implying that the R316Q mutation did not have any affect on FTO stability.

2D-DIGE Analysis of the WT and the Mutant FTO Expressing SH-SY5Y Cells

Protein isolation from each created stable cell line (FTO-WT SH-SY5Y cell lines #3, #5, #12; FTO-R316Q SH-SY5Y cell lines #2, #3, #5) was performed. An equal amount of protein was taken from each samples where protein concentrations were measured, and protein pools were created. Each protein pools were labeled as the WT-FTO-ind and the R316Q-FTO-ind for Tet-induced samples, and the WT-FTO-unind and the R316Q-FTO-unind for uninduced samples. 2D-DIGE experiments were performed with these pooled samples. The pooled samples were then labelled with Cy2, Cy3 and Cy5 according to the instructions provided by the supplier (Life Tech, USA) (Table 1). To monitor the changes observed at the proteome level well-resolved DIGE gels were generated from the soluble protein extracts prepared from FTO expressing and non-expressing cells (Figure 5A). Analysis of DIGE images using spot detection tool revealed 500 (±20) spots per gel. Protein spots were compared based on the 2-fold regulation criteria. Superimposition of the gel images using PDQuest Advance revealed the presence of six differentially expressed proteins among the protein extracts. In overall, the expression of neither the WT nor the mutant FTO caused any major changes in the soluble proteome. However, we observed some minimal changes (less than three-fold) in six protein spots. The minimally regulated spots were excised from the preparative gels via ExQuest Spot cutter into a 96-well plate and successfully identified with MALDI-TOF/TOF analysis. Spots positions of the excised proteins on the preparative gel were shown in Figure 5B. The identified proteins listed in Table 2 were Heat shock protein 70-1A (Hsp70-1A), Phosphoglycerate kinase-1 (PGK1), Calmodulin and Keratin. Three of the identified protein spots belonged to the same protein, Hsp70. The regulation ratios and trends of the identified proteins according to 2-fold regulation criteria were given in Table 3. The mutant protein overexpressing caused up-regulation of Hsp70 and Calmodulin while overexpressing WT-FTO protein caused up-regulation of Calmodulin and down-regulation of Keratin in comparison to the control cells. Comparisons were also performed between the WT and the mutant FTO overexpressing SH-SY5Y cell-free extracts. Calmodulin was up-regulated and PGK1 and Keratin were down-regulated in the WT-FTO protein overexpressing cells. The close up 3D images for the regulated proteins were presented in Figure 6. Western blot analysis was performed to validate the differential expression of Hsp70. The results indicated that the observed regulation represented the actual changes that occurred at the proteome level (Figure 7).

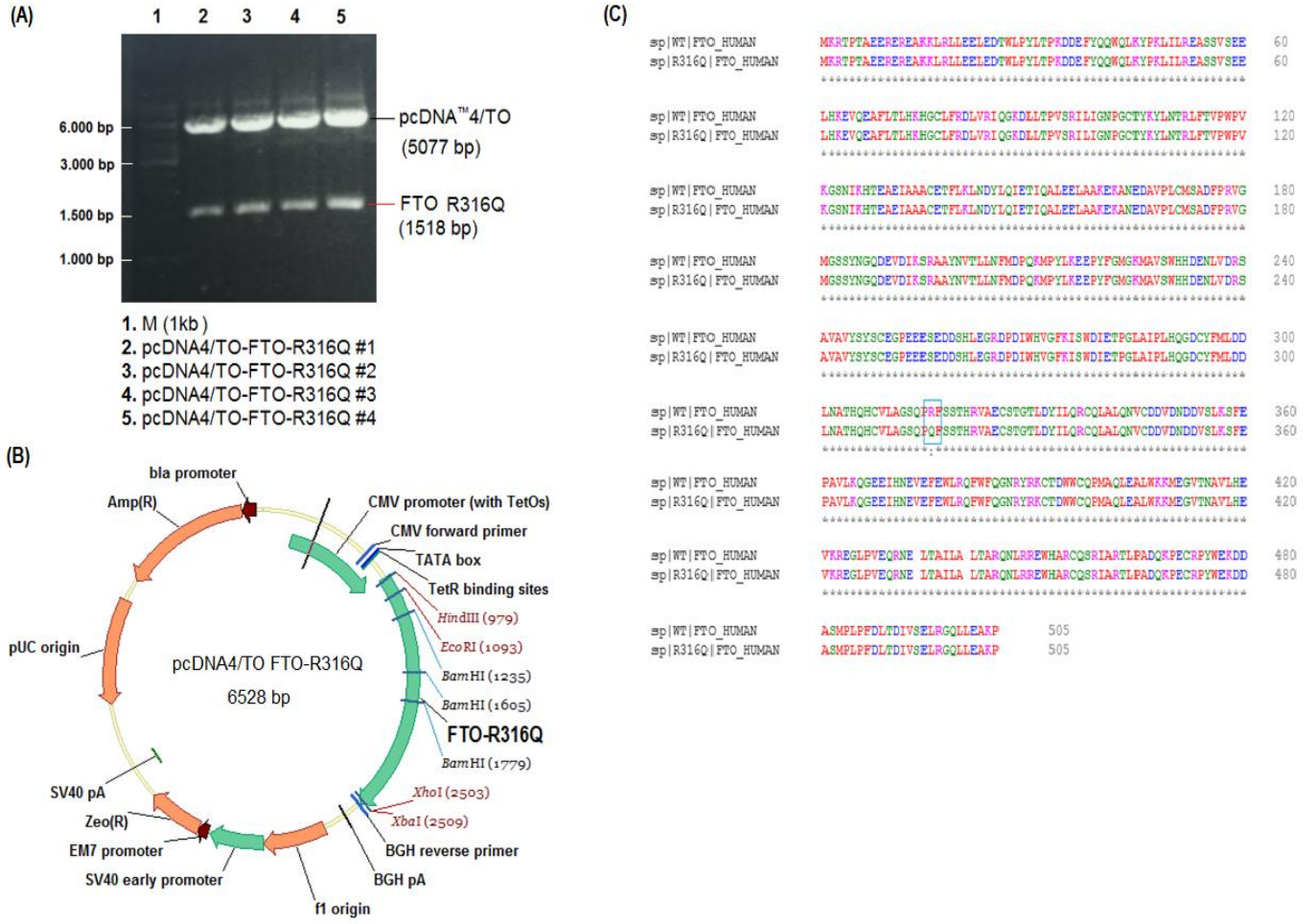

Figure 1. Representation of cloning strategy using FTO R316Q clone. A) Agarose gel image for insert and vector visualization after double digest with HindIII and XhoI restriction enzymes. Lane 1 shows the gene ruler 1 Kb DNA ladder (Thermo Fisher Scientific, USA), Lane 2, 3, 4 and 5 show the digested form of pcDNA4/TO-FTO-R316Q to demonstrate the presence of 1518 bp insert. B) In silico map for pcDNA4/TO-FTO-R316Q clone. The map was prepared with Vector NTI (Invitrogen, USA). C) Comparison using the multiple sequence alignment program of the wild type and the mutant type FTO sequences.

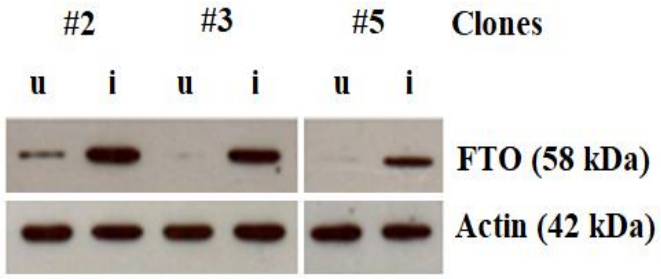

Figure 2. Western blots analysis for colony screening to determine the wild- type FTO expression under tetracycline control. 20 µg proteins per lane were loaded from each sample. The blot was blotted with a monoclonal anti-FTO antibody (SantaCruz, USA), stripped and then reprobed with a monoclonal anti-beta actin antibody (SantaCruz, USA).

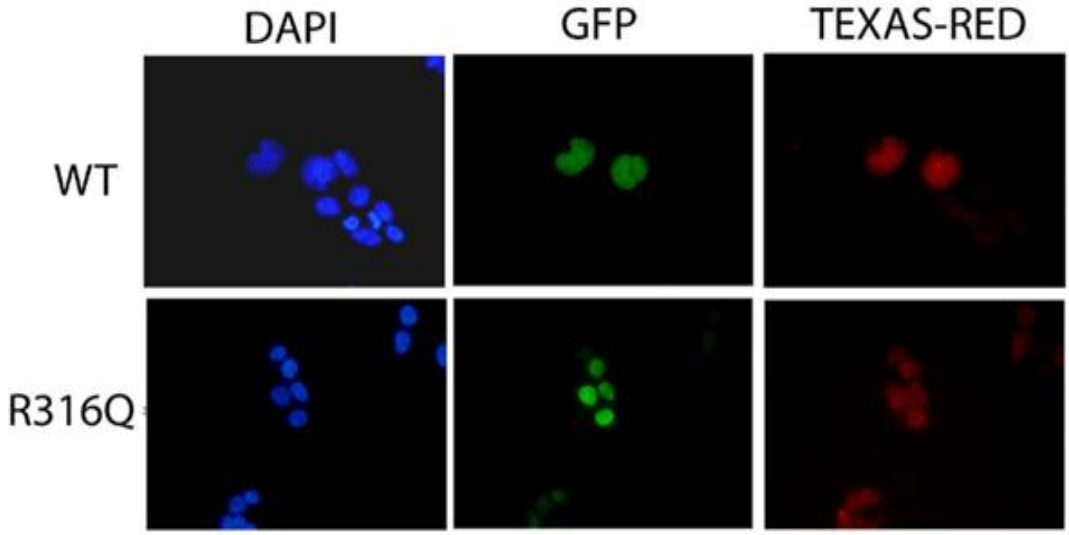

Figure 3. Immunofluorescence microscopy analysis of cells expressing the WT and the mutants GFP-FTO fusion proteins. An anti-FTO monoclonal primary antibody (1:100) and a Texas Red-conguated anti-mouse secondary antibody (1:100) were used. The cell nucleus is stained with DAPI (1:20.000)(blue).

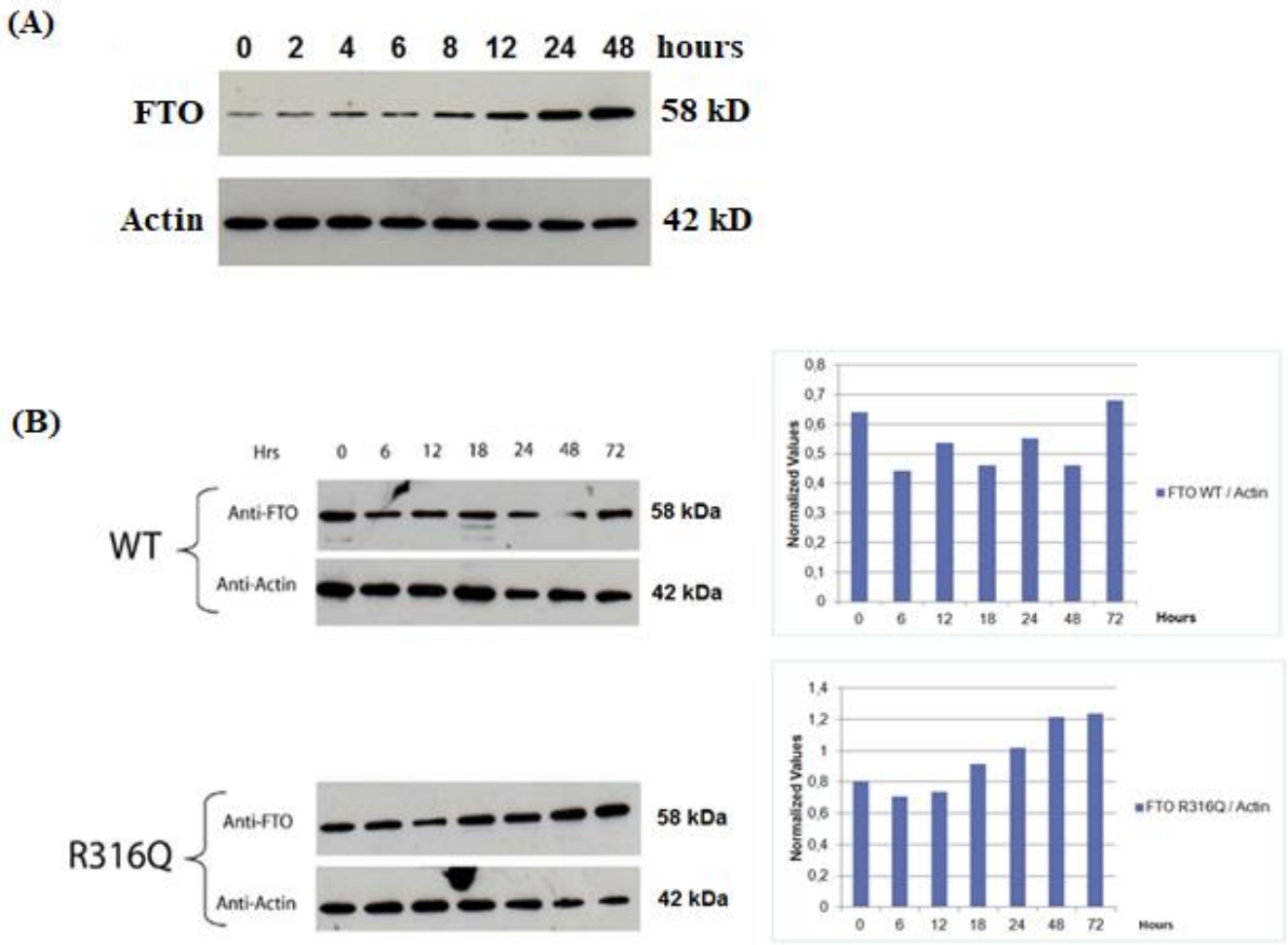

Figure 4. Western blot analysis of the cell-free extracts prepared from cells collected during cyclohexamide chase experiments of the WT and the mutants FTO proteins. A) Time-dependent expression levels of FTO after tetracycline induction of SH-SY5Y-FTO-WT cells. 15 µg of protein was loaded into each well. B) The stability of FTO proteins for a specific time course. Primary antibodies were anti-FTO (1: 1,000) and anti-actin (1:1,000), the secondary antibody was HRP-conjugated anti-mouse (1: 20,000). Actin was used as a loading control.

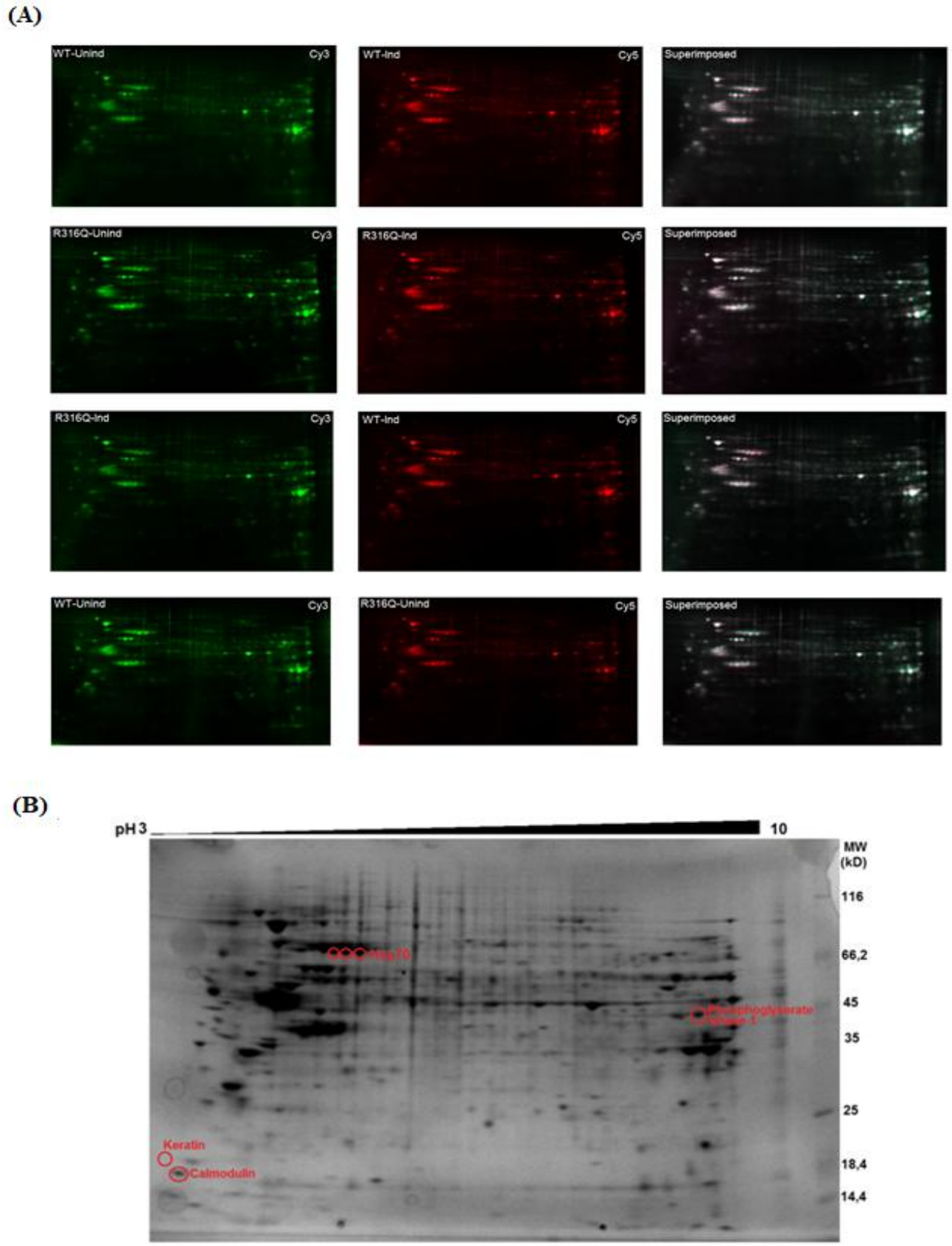

Figure 5. Representative 2D images of the gels. A) DIGE analysis of the cells expressing either the WT or the mutant (R316Q) FTO proteins. The proteins were labelled with Cy3(Green), Cy5(Red) and Cy2(Blue) fluorescent dyes. The images were superimposed to reveal the changes in protein expression levels. B) The positions for the identified protein spots on the preparative gel.

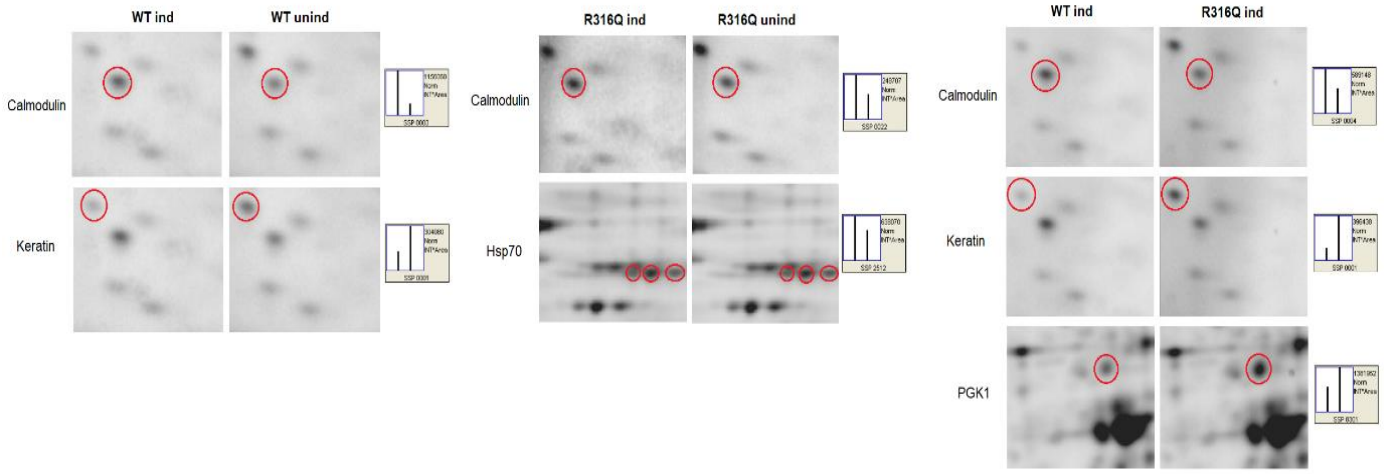

Figure 6. The close-up images of the regulated protein spots and their corresponding spot intensities. Relative quantification of the spots was performed using PD Quest Advanced software (BioRad, USA). ind refers to cells overexpressing the FTO protein by adding tetracycline to the cell culture. unind refers to cells that do not overexpress the FTO protein.

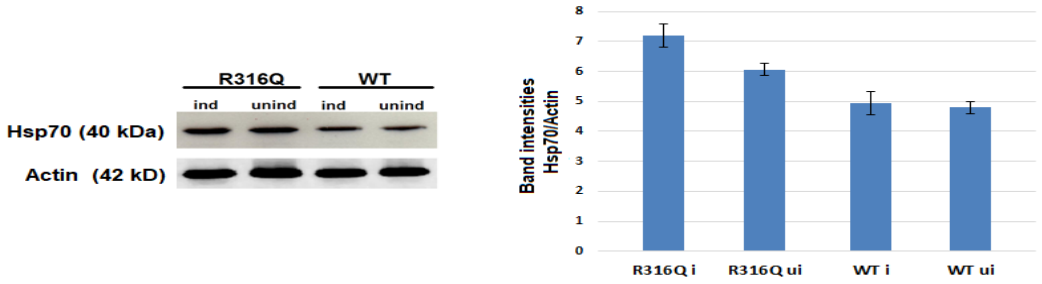

Figure 7. Western blot analysis of Hsp70 expression in the mutant pcDNA4/TO-FTO-R316Q and the wild type pcDNA4/TO-FTO-WT expressing cells. The bar graph was created using the intensity values of the bands obtained from ImageJ.

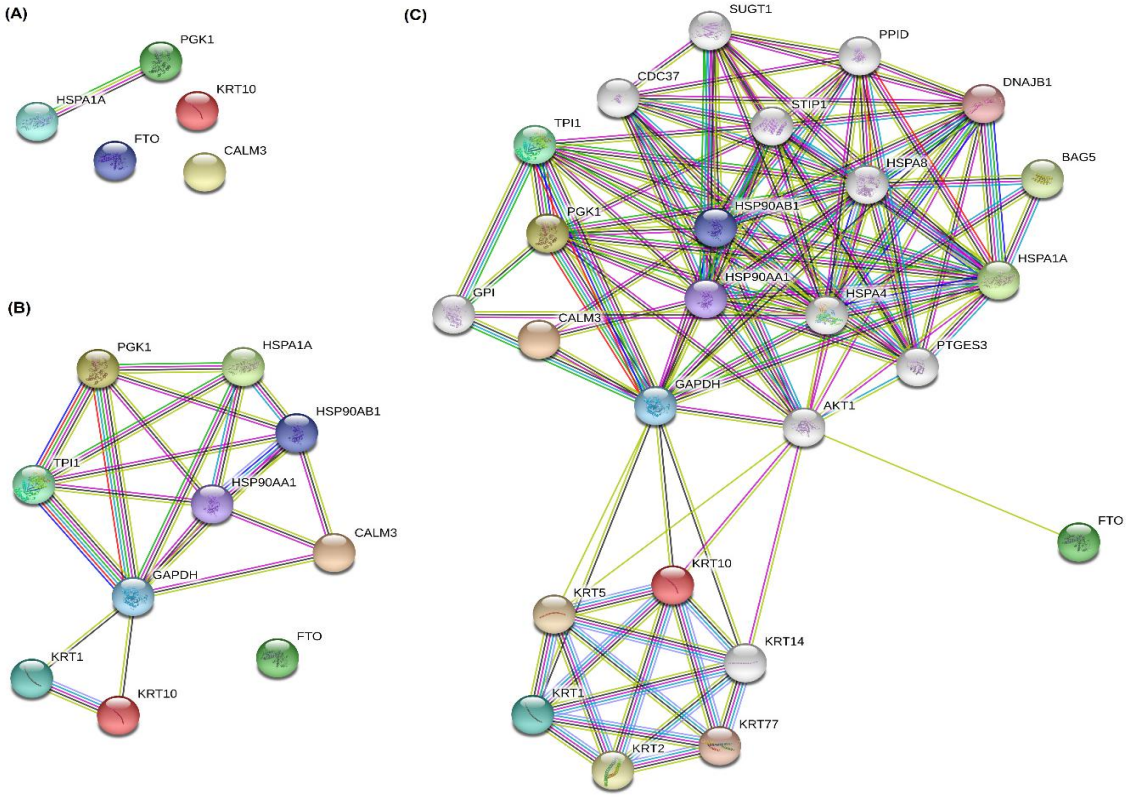

Figure 8. STRING analysis of identified proteins and FTO interactions. A) The STRING analysis with high confidence and no consideration of maximum number of interactions in the first and second shells. B) The STRING analysis with decreased stringency using the settings of maximum number of interactions 5 in the first shells and considering all the possible interaction sources provided by the database. C) The STRING analysis with high confidence and with all the active interaction sources considered. Ten was set as the maximum number of interactions on the first and second shells. The abbreviations stand for the following: FTO: fat mass and obesityassociated protein, PGK1: phosphoglycerate kinase 1 HSPA1A: Heat shock 70 kD protein 1A/1B CALM3: Calmoduline, KRT10: Keratin, type I cytoskletal 10.

Table 1. Experimental set up for differential labeling of cell-free extracts for DIGE analysis. a. Internal controls were created by mixing equal amount of samples and used for normalization. cfe: cell free extract

Gel No.	CyDye used (Cy3)	CyDye used (Cy5)	CyDye used (Cy2) [a]
1	WT-FTO unind.- *cfe*	WT-FTO ind.- *cfe*	Int. control
2	R316Q-FTO unind.- *cfe*	R316Q-FTO ind.- *cfe*	Int. control
3	R316Q-FTO ind.- *cfe*	WT-FTO ind.- *cfe*	Int. control
4	WT-FTO unind.- *cfe*	R316Q-FTO unind.- *cfe*	Int. control

Table 2. Proteins identified by MALDI-TOF/TOF analysis

SSP No	Swiss-Prot Acc. No.	Best Prot. Acc. No.	Best Prot. Mass	Protein Score	Exp. score	Matches	Calc. pI	Seq. Cov. (%)	Best Protein Description	Matched Peptide w/highest score
0003	P62158	CALM_HUMAN	16824	157	3E-012	12	4,57	44	Calmodulin	K.DTDSEEEIREAFR.V R. VFDKDGNGYISAAELR.H K.EAFSLFDKDGDGTITTK.E
2512	P0DMV8 (HS71A_HUMAN) and P0DMV9 (HS71B_HUMAN)	HSP71_HUMAN (Demerged into P0DMV8 and P0DMV9)	70009	516	5,1E-048	32	4,73	36	Heat shock 70 kD protein 1A/1B	K.ITITNDKGR.L K.LLQDFFNGR.I K.DAGVIAGLNVLR.I R.FEELCSDLFR.S + Carbamidomethyl (C) R.LVNHFVEEFKR.K K.AQIHDLVLVGGSTR.I R.TTPSYVAFTDTER.L R.ARFEELCSDLFR.L + Carbamidomethyl(C) K.ATAGDTHLGGEDFDNR.L R.IIINEPTAAAIAYGLDR.T
8301	P00558	PGK1_HUMAN	44586	181	1,6E-014	18	8,15	40	Phospfogliserate kinase 1	K.YAEAVTR.A K. LGDVYVNDAFGTAHR.A K.ACANPAAGSVILLENLR.F + Carbamidomethyl (C)
0001	P13645	K1C10_HUMAN	58792	165	6,4E-013	17	4,73	27	Keratin, type I cytoskletal 10	K.YEELQITAGR.H

Table 3. Regulation ratios and trends of the identified proteins. Rr.: Regulation ratio, Rt.: Regulation trend, nr: not regulated.

Protein names	R316Q i / R316Q ui		WT i / WT ui		WT i / R316Q i		WT ui / R316Q ui	
	Rr	Rt	Rr	Rt	Rr	Rt	Rr	Rt
PGK1	nr	Nr	nr	nr	0,57	Down	nr	nr
Calmodulin	2,36	Up	2,72	Up	2,78	Up	nr	nr
Hsp70	2,76	Up	nr	nr	nr	nr	nr	nr
Keratin	nr	Nr	0,51	Down	0,28	Down	nr	nr

Discussion

The power of modifying mRNA structure by post-transcriptional modification places a significant multi-functional role on FTO.[4,7-9] One of the reflections of such activity linked FTO to obesity. Researchers found a direct link between FTO mutations and obesity.[12-15] Further research elucidated more about the physiological role of FTO and revealed that FTO is not only associated with obesity but also with a seemingly unrelated disorder, neurodegeneration.[16-21] However, so far no direct link was provided regarding the mechanism for the effect of FTO on neuronal degeneration. In this study, we choose to study the effect of expressing the WT and the mutant FTO expressions on the soluble proteome of SH-SY5Y cells. The mutant that we picked causes complete loss of FTO activity and thus expected to have a significant impact on the proteome.[22] We created cell lines that allowed controlled expression of both the WT and the mutant FTO proteins to precisely monitoring of the changes occurring on cellular proteome. After induction of the protein synthesis, significant increases were observed in the levels of the WT and the mutant FTO proteins indicating that exogenous expression of both proteins are sufficient to monitor the changes. The SH-SY5Y cells that we used in this study had a basal level of FTO expression as it was evident from the western blots. However, this type expression level did not prevent the effect of the mutant FTO on cellular proteome considering the fact that the R316Q mutation is a dominant negative mutation that might act antagonistically to the WT protein.

The stable cell cultures that were created in this study provided additional strength to the findings since the cells were not placed under a stress of transient transfection conditions. Not only that but also we screened three different monoclonal clones to monitor the effect of each protein and minimize clone to clone variation. In most studies using tet-regulated protein expression systems, a single stable clone is used without considering the fact that differences may occur between different clones.[31] Therefore, the results provided here were highly confident in providing a snapshot of the changes that occurred during expressions of the WT and the mutant FTO proteins.

The overall evaluation of the data implicated that the soluble proteome of SH-SY5Y cells were not profoundly affected by the expressions of the WT or the mutant FTO proteins. In particular, the expression did not prevent or induce synthesis of a specific protein (s) since there were no spots on 2DE gels that disappeared or appeared after the induction of the mutant FTO. However, minimal changes occurred in expression levels of some proteins implying that the expression of the WT and the mutant FTO did have an indirect effect on the soluble proteome. The changes at the levels of Hsp70, PGK1, Calmodulin and Keratin were worthy of consideration and thus were further discussed.

Heat shock protein 70-1A (Hsp70-1A) is the major stress-inducible member of the HSP70 chaperone family and also known as HSPA1A, Hsp70-1, Hsp72, or HSPA1.[35,36] Heat shock protein 70-1A acts as a central component of the cellular network of molecular chaperones and folding catalysts inside cells. Its ectopic expression confers protection against stresses that induce protein damage, e.g. heat, ischemia and oxidative stress in cultured cells.[37,38] Previous studies showed changes in Hsp70 levels in FTO knockdown cells[39] and heat stress increased expression of genes involved in lipogenesis.[40] The increased levels of Hsp70 in the mutant induced cultures indicated that the mutant FTO expression induced changes in Hsp70 involved metabolic activities. In our MALDI-TOF/TOF analysis, several protein spots cut from different regions of the gels were identified to belong to the Hsp70. This observation implicated that Hsp70 was post-translationally modified upon FTO expression and thus positioned itself in several different locations on the gels.

Phosphoglycerate kinase-1 (PGK1) is present in all living organisms as one of the two ATP-generating enzymes of glycolysis. It catalyzes the reversible transfer of a phosphate group from 1,3-bisphosphoglycerate (1,3-BPG) to ADP producing 3-phosphoglycerate (3-PG) and ATP. In gluconeogenesis, PGK1 catalyzes the reverse reaction, generating ADP and 1,3-BPG.[41] Two recent studies reported that FTO affects energy metabolism (glycolysis and gluconeogenesis) of chicken embryo fibroblast cells and breast cancer cells.[42,43] In our study, a change in the regulation of PGK1 protein was observed only in the experiments that compared the samples overexpressing the mutant and the wild-type FTO proteins. The mutant FTO expression caused up-regulation of up-to 2-fold overexpression of PGK1 compared to the wild-type protein overexpressed cells. The differential regulation that was observed in PGK1 levels might be due to the effect of the FTO on energy metabolism.

Calmodulin which mediates many crucial processes such as inflammation, metabolism, apoptosis, smooth muscle contraction, intracellular movement, short-term and long-term memory, and the immune response is a multifunctional intermediate calcium-binding messenger protein and expressed in all eukaryotic cells.[44] Lin et al (2014) discovered an interaction between FTO and Calcium/calmodulin-dependent protein kinase II (CaMKII) by yeast hybridization.[45] Osborne et al (2014) identified that FTO as a protein-regulator of the balanced activation between canonical and non-canonical branches of the Wnt pathway and presented that it plays a role in development and cilia formation/function. They even attributed a role to the FTO as a protein regulator of the balanced activation between canonical and non-canonical branches of the Wnt pathway.[46] We observed an increase in Calmodulin expression in the samples where both the wild and the mutant FTO proteins were overexpressed. However, the expression level of calmodulin in the WT-FTO expressing samples was higher than in the mutant FTO expressing samples. Our findings regarding the changes in the Calmodulin levels upon expression of either the WT and or the mutant FTO proteins in the cells support the know-how that FTO balances the activation between canonical and non-canonical branches of the Wnt pathway.

Keratin-10 (KRT10), also known as cytokeratin-10 (CK-10), is an intermediate filament (IF) chain which belongs to the acidic type I family. It is a structural protein which is expressed by terminally differentiated epidermal cells. These filaments, along with actin microfilaments and microtubules, compose the cytoskeleton of epithelial cells.[47,48] In previous studies, KRT10 has been reported to be involved in the inhibition of cell-cycle progression and keratinocyte proliferation.[49-51] In our study, downregulation of Keratin-10 was observed only in the WT-FTO overexpressing cells. Keratin-type proteins play roles in various parts of the cells due their structural properties and thus can be correlated with many metabolic events. However, we speculate that the downregulation of Keratin-10, upon FTO expression may occur via AKT signaling pathway since STRING analysis connected FTO to Keratin10 via AKT1 (Figure 8C). In the literature, Keratin-10 has been shown to interact with AKT1.[52]

To predict the interaction partners of FTO using the differentially regulated proteins identified in this study, we performed STRING analysis. Initial analysis using high stringency with no first and second shell application failed to create a definitive interactome among the differentially regulated proteins (Figure 8A). When stringency was lowered by expanding the first and second shell interacting proteins to a number of five we were able to create an interactome among differentially regulated proteins except FTO (Figure 8B). Finally, by expanding the first and second shell interacting proteins to a number of ten, a dynamic interaction map was created (Figure 8C). The analysis of the STRING results revealed the presence of several statistically significant biological processes, including the changes in carbon and amino acid metabolisms as well as the changes in protein processing in endoplasmic reticulum. In addition, there were several differentially regulated proteins belonged to HIF-1 signalling pathway and PI3K-Akt signalling pathway. The literature search regarding FTO protein revealed that the levels of some of the proteins associated with carbon metabolism changes and PI3K/Akt signaling pathway. One of these proteins plays role in glycolysis or glyconeogenessis (PGK1), while two of them display activity in estrogen signalling pathway (HSPA1A and KRT10). HSPA1A is also associated with protein processing in endoplasmic reticulum and antigen processing and presentation. STRING analysis using KEGG, no correlation was found for Calmodulin. In STRING analysis using biological processes and metabolic pathways, HSPA1A was associated with chaperone-mediated protein

complex assembly and protein folding, PGK1 was associated with glycolysis and gluconeogenesis, and PGK1 and CALM3 were associated with phosphorylation.

Recent studies demonstrated that FTO regulates the proliferation and differentiation of 3T3-L1 cells via multiple mechanisms, including PPARγ and PI3K/Akt signaling[53] and that decreased RNA m6A methylation levels as a result of overexpression of FTO in different types of cancer might activate Wnt/PI3K-Akt signaling pathway.[43,54,55] The reported findings in the literature justifies the fact that FTO overexpression may stimulate various changes in cells via triggering different metabolic events. The findings of this study, especially underlined this fact and stimulated us to carry out further studies regarding elucidation of FTO associated/affected pathways and interactomes. Revealing such information should provide novel tools that may have use in diagnosis, prognosis and therapy of various diseases, including cancer.

Study Limitation

The findings of this study represent changes occuring in *in vitro*. These changes should be verified in *in vivo* models. The findings of this study was reflection of a snapshot changes in cellular proteome upon FTO expression. A time-dependent FTO expression should also be studied.

Acknowledgements

The authors would like to thank the TUBİTAK, which contributed to the study (Project No: SBAG-113S965)

Conflict of Interest

All authors declare no conflict of interest.

Author Contribution

AK: Critical revision; data analysis and interpretation; data collection; literature search, resources, materials; manuscript drafting/writing/editing; study design and conception; MK: Critical revision; data analysis and interpretation; data collection; literature search, resources, materials; manuscript drafting/writing/editing; study design and conception; supervision; GA: Critical revision; data analysis and interpretation; SY: Data collection; literature search, resources, materials.

References

1. Gerken T, Girard CA, Tung YC, et al. The obesity-associated FTO gene encodes a 2-oxoglutarate-dependent nucleic acid demethylase. *Science*. 2007;318:1469-1472.
2. Sanchez-Pulido L and Andrade-Navarro MA. The FTO (fat mass and obesity associated) gene codes for a novel member of the non-heme dioxygenase superfamily. *BMC Biochem*. 2007;8:23.
3. Jia G, Yang CG, Yang S, et al. Oxidative demethylation of 3-methylthymine and 3-methyluracil in single-stranded DNA and RNA by mouse and human FTO. *FEBS Lett*. 2008;582:3313–3319. doi:10.1016/j.febslet.2008.08.019.
4. Jia G, Fu Y, Zhao X, et al. N6-Methyladenosine in nuclear RNA is a major substrate of the obesity-associated FTO. *Nat. Chem. Biol*. 2011;7:885–887. doi:10.1038/nchembio.687.
5. Gulati P, Cheung MK, Antrobus R, et al. Role for the obesity-related FTO gene in the cellular sensing of amino acids. *Proc. Natl. Acad. Sci. U.S.A.* 2013;110:2557–2562. doi:10.1073/pnas.1222796110.
6. Gulati P, Avezov E, Ma M, et al. Fat mass and obesity-related (FTO) shuttles between the nucleus and cytoplasm. *Biosci Rep*. 2014;34:e00144. doi:10.1042/BSR20140111.
7. Meyer KD, Saletore Y, Zumbo P, Elemento O, Mason CE, Jaffrey SR. Comprehensive Analysis of mRNA Methylation Reveals Enrichment in 3' UTRs and near Stop Codons. *Cell*. 2012;149:1635–1646. doi:10.1016/j.cell.2012.05.003.
8. Xiang Y, Laurent B, Hsu Nachtergaele S, et al. RNA m(6)A methylation regulates the ultraviolet-induced DNA damage response. *Nature*. 2017;543:573-576. doi:10.1038/nature21671.
9. Geula S, Moshitch-Moshkovitz S, Dominissini D, et al. Stem cells. m6A mRNA methylation facilitates resolution of naïve pluripotency toward differentiation. *Science*. 2015;347:1002-1006. doi:10.1126/science.1261417.
10. Mauer J, Luo X, Blanjoie A, et al. Reversible methylation of m(6)Am in the 5′cap controls mRNA stability. *Nature*. 2017;541:371–375. doi:10.1038/nature21022.
11. Wei J, Liu F, Lu Z, et al. Differential m(6)A, m(6)Am, and m(1)A demethylation mediated by FTO in the cell nucleus and cytoplasm. *Mol Cell*. 2018;71:973–985. doi:10.1016/j.molcel.2018.08.011.
12. Dina C, Meyre D, Gallina S, et al. Variation in FTO contributes to childhood obesity and severe adult obesity. *Nat Genet*.2007;39:724–726.
13. Frayling TM, Timpson NJ, Weedon MN, et al. A common variant in the FTO gene is associated with body mass index and predisposes to childhood and adult obesity. *Science*.2007;316:889–894.
14. Scuteri A, Sanna S, Chen WM, et al. Genome-wide association scan shows genetic variants in the FTO gene are associated with obesity-related traits. *PLoS Genet.* 2007;3:115.
15. Meyre D, Proulx K, Kawagoe-Takaki H, et al. Prevalence of loss-of-function FTO mutations in lean and obese individuals. *Diabetes*. 2010;59:311–318. doi:10.2337/db09-0703.
16. Rivera M, Cohen-Woods S, Kapur K, et al. Depressive disorder moderates the effect of the FTO gene on body mass index. *Mol Psychiatry*. 2012;17:604-611. doi:10.1038/mp.2011.45.
17. Keller L, Xu W, Wang HX, Winblad B, Fratiglioni L, Graff C. The obesity related gene, FTO, interacts with APOE, and is associated with Alzheimer's disease risk: a prospective cohort study. *J Alzheimers Dis*. 2011;23:461-469. doi:10.3233/JAD-2010-101068.
18. Reitz C, Tosto G, Mayeux R, Luchsinger JA. NIA-LOAD/NCRAD Family Study Group; Alzheimer's Disease Neuroimaging Initiative. Genetic variants in the Fat and Obesity Associated (FTO) gene and risk of Alzheimer's disease. *PLoS One*. 2012;7:e50354. doi:10.1371/journal.pone.0050354.
19. Rowles J, Wong M, Powers R, Olsen M. FTO, RNA epigenetics and epilepsy. *Epigenetics*. 2012;7:1094-1097. doi:10.4161/epi.21977.
20. Mitropoulos K, Merkouri Papadima E, Xiromerisiou G, et al. Genomic variants in the FTO gene are associated with sporadic amyotrophic lateral sclerosis in Greek patients. *Hum Genomics*. 2017;11:30. doi:10.1186/s40246-017-0126-2.
21. Chang JY, Park JH, Park SE, Shon J, Park YJ. The Fat Mass-and Obesity-Associated (FTO) Gene to Obesity: Lessons from Mouse Models. *Obesity (Silver Spring)*. 2018;26:1674-1686. doi:10.1002/oby.22301.
22. Boissel S, Reish O, Proulx K, et al. Loss-of-function mutation in the dioxygenase-encoding FTO gene causes severe growth retardation and multiple malformations. *Am J Hum Genet*. 2009;85:106–111. doi:10.1016/j.ajhg.2009.06.002.
23. Gao X, Shin YH, Li M, Wang F, Tong Q, Zhang P. The fat mass and obesity associated gene FTO functions in the brain to regulate postnatal growth in mice. *PLoS One*. 2010;5:e14005. doi:10.1371/journal.pone.0014005.
24. Zhao X, Yang Y, Sun BF, Zhao YL, Yang YG. FTO and Obesity: Mechanisms of Association. *Curr Diab Rep*. 2014;14:486. doi:10.1007/s11892-014-0486-0.
25. Kasap M, Akpinar G, Kanli A. Proteomic studies associated with Parkinson's disease. *Expert Rev Proteomics*. 2017;14:193-209. doi:10.1080/14789450.2017.1291344.
26. Kanli A, Kasap M, Akpinar G, Gulkac MD. Comparative analysis of glucoprotein profiles of SH-SY5Y cells stably

expressing the wild type fat mass and obesity associated proteins. *TJMBB*. 2017;2:10–20.
27. Guzel N, Kasap M, Kanli A, Akpinar G, Gulkac MD, Karaosmanoglu K. Exogenous Expressions of FTO Wild-Type and R316Q Mutant Proteins Caused an Increase in HNRPK Levels in 3T3-L1 Cells as Demonstrated by DIGE Analysis. *Biomed Res Int*. 2017;2017:8216180. doi:10.1155/2017/8216180.
28. Rennel E, Gerwins P. How to make tetracycline-regulated transgene expression go on and off. *Anal Biochem*. 2002;309:79–84.
29. Ozgul S, Kasap M, Akpinar G, Kanli A, et al. Linking a compound-heterozygous Parkin mutant (Q311R and A371T) to Parkinson's disease by using proteomic and molecular approaches. *Neurochem Int*. 2015;85–86:1–13. doi:10.1016/j.neuint.2015.03.007.
30. Kasap M, Akpinar G, Guzel N, Selimoglu M. Stable expression of human proteins in cultured cells. *TJMBB*. 2016;1:72–79.
31. Kanli A, Kasap M, Yoneten KK, Akpinar G, Gulkac MD. Identification of differentially regulated deceitful proteins in SH-SY5Y cells engineered with Tet-regulated protein expression system. *J Cell Biochem*. 2018;119:6065-6071. doi:10.1002/jcb.26804.
32. Kasap M, Thomas S, Danaher E, Holton V, Jiang S, and Storrie B. Dynamic nucleation of Golgi apparatus assembly from the endoplasmic reticulum in interphase HeLa cells. *Traffic*. 2004;5:595–605.
33. Kasap M, Yegenaga I, Akpinar G, Tuncay M, Aksoy A, and Karaoz E. Comparative proteome analysis of hAT-MSCs isolated fromchronic renal failure patients with differences in their bone turnover status. *PLoS ONE*. 2015;10:e0142934. doi:10.1371/journal.pone.0142934.
34. Kasap M, Torol S, Gacar G, and Budak F. Ethidium bromide spot test is a simple yet highly accurate method in determining DNA concentration. *Turkish Journal of Medical Sciences*. 2006;36:383–386.
35. Kampinga HH, Hageman J, Vos MJ, et al. Guidelines for the nomenclature of the human heat shock proteins. *Cell Stress Chaperones*. 2009;14:105-111 doi:10.1007/s12192-008-0068-7.
36. Radons J. The human HSP70 family of chaperones: where do we stand? *Cell Stress Chaperones*. 2016;21:379-404. doi:10.1007/s12192-016-0676-6.
37. Lindquist S, Craig EA. The heat-shock proteins. *Annu. Rev. Genet.* 1988;22:631-677. doi:10.1146/annurev.ge.22.120188.003215.
38. Daugaard M, Rohde M, Jaattela M. The heat shock protein 70 family: highly homologous proteins with overlapping and distinct functions. *FEBS Lett*. 2007 581:3702-3710. doi:10.1016/j.febslet.2007.05.039.
39. Zhou J, Wan J, Gao X, Zhang X, Jaffrey SR, Qian SB. Dynamic m6A mRNA methylation directs translational control of heat shock response. *Nature*. 2015;526:591–594. doi:10.1038/nature15377.
40. Heng J, Tian M, Zhang W, Chen F, Guan W, Zhang S. Maternal heat stress regulates the early fat deposition partly through modification of m6A RNA methylation in neonatal piglets. *Cell Stress Chaperones*. 2019;24:635-645. doi:10.1007/s12192-019-01002-1.
41. Watson HC, Walker NP, Shaw PJ, et al. Sequence and structure of yeast phosphoglycerate kinase. *The EMBO Journal*. 1982;1:1635–1640.
42. Guo F, Zhang Y, Zhang C, Wang S, Ni Y, Zhao R. Fat mass and obesity associated (FTO) gene regulates gluconeogenesis in chicken embryo fibroblast cells. *Comp Biochem Physiol A Mol Integr Physiol*. 2015;179:149-156.
43. Liu Y, Wang R, Zhang L, Li J, Lou K, Shi B. The lipid metabolism gene FTO influences breast cancer cell energy metabolism via the PI3K/AKT signaling pathway. *Oncol Lett*. 2017;13:4685-4690. doi:10.3892/ol.2017.6038.
44. Stevens, FC. Calmodulin: an introduction. *Can J Biochem Cell Biol*. 1983;61:906–910. doi:10.1139/o83-115.
45. Lin L, Hales CM, Garber K, Jin P. Fat mass and obesity-associated (FTO) protein interacts with CaMKII and modulates the activity of CREB signaling pathway. *Hum Mol Genet*. 2014;23:3299-3306. doi:10.1093/hmg/ddu043.
46. Osborn DP, Roccasecca RM, McMurray F, Hernandez-Hernandez V, Mukherjee S, Barroso I, et al. Loss of FTO antagonises Wnt signaling and leads to developmental defects associated with ciliopathies. *PLoS One*. 2014;9:e87662. doi:10.1371/journal.pone.0087662.
47. Schweizer J, Bowden PE, Coulombe PA, et al. New consensus nomenclature for mammalian keratins. *J Cell Biol*. 2006;174:169-174. doi:10.1083/jcb.200603161
48. UniProtKB - P13645 (K1C10_HUMAN). https://www.uniprot.org/uniprot/P13645. Accessed September 22, 2019.
49. Paramio JM, Casanova ML, Segrelles C, Mittnacht S, Lane EB, Jorcano JL. Modulation of cell proliferation by cytokeratins K10 and K16. *Mol Cell Biol*. 1999;19:3086-3094. doi:10.1128/mcb.19.4.3086.
50. Magin TM, Vijayaraj P, Leube RE. Structural and regulatory functions of keratins. *Exp Cell Res*. 2007;313:2021-2032. doi:10.1016/j.yexcr.2007.03.005.
51. Reichelt J, Breiden B, Sandhoff K, Magin TM. Loss of keratin 10 is accompanied by increased sebocyte proliferation and differentiation. *Eur J Cell Biol*. 2004;83:747-759. doi:10.1078/0171-9335-00429.
52. Paramio JM, Segrelles C, Ruiz S, Jorcano JL. Inhibition of protein kinase B (PKB) and PKCzeta mediates keratin K10-induced cell cycle arrest. *Mol Cell Biol*. 2001;21:7449-7459. doi:10.1128/MCB.21.21.7449-7459.2001.
53. Jiao Y, Zhang J, Lu L, Xu J, Qin L. The Fto Gene Regulates the Proliferation and Differentiation of Pre-Adipocytes in Vitro. *Nutrients*. 2016;8(2):102. doi:10.3390/nu8020102.
54. Zhang Z, Zhou D, Lai Y, et al. Estrogen induces endometrial cancer cell proliferation and invasion by regulating the fat mass and obesity-associated gene via PI3K/AKT and MAPK signaling pathways. *Cancer Lett*. 2012;319(1):89-97. doi:10.1016/j.canlet.2011.12.033.
55. Zhang C, Zhang M, Ge S, et al. Reduced m6A modification predicts malignant phenotypes and augmented Wnt/PI3K-Akt signaling in gastric cancer. *Cancer Med*. 2019;8:4766-4781. doi:10.1002/cam4.2360.